11. V. M. Möhring and G. Fink, *Angew. Chem. Int. Ed. Engl.* **24**, 1001 (1985).
12. S. J. McLain *et al.*, *Polymer Prep.* **38** (no. 1), 772 (1997).
13. A typical polymerization was done as follows: A solution of 50 mg (33.9 μmol) of the Pd-α-dimine catalyst in 100 ml of chlorobenzene was transferred into a 600-ml Parr pressure reactor under nitrogen. The reactor was heated to 35°C, and the solution was stirred by a mechanical stirrer set at 500 rpm. The reactor was pressurized with ethylene to 101.3 kPa. Polymerization was continued at 35°C and 101.3 kPa for 18.7 hours. After termination of the polymerization, the solution was diluted with toluene, then passed through a column packed with alumina, silica gel, and Celite to remove the catalyst, and finally precipitated into a large excess of methanol. The polymer was collected and dried in vacuo to give 15.8 g of PE as viscous oil.
14. P. J. Flory, *Principles of Polymer Chemistry* (Cornell Univ. Press, Ithaca, NY, 1953).
15. D. A. Tomalia, A. M. Naylor, W. A. Goddard III, *Angew. Chem.* **102**, 119 (1990).
16. Z. Xu *et al.*, *Macromolecules* **18**, 2560 (1985).
17. W. Burchard, *Adv. Polym. Sci.* **48**, 1 (1983).
18. B. J. Bauer, L. J. Fetters, W. W. Graessely, N. Hadjichristidis, G. F. Quack, *Macromolecules* **22**, 2337 (1989).
19. D. Kunz, A. Thurn, W. Burchard, *Polym. Coll. Sci.* **261**, 635 (1983).
20. R. Scherrenberg *et al.*, *Macromolecules* **31**, 456 (1998).
21. M. S. Brookhart, D. J. Tempel, L. K. Johnson, unpublished data.
22. We thank M. S. Brookhart, L. K. Johnson, M. Spinu, S. D. Ittel, L. Wang, Z. Yang, P. Soper, and S. D. Arthur for helpful discussions; R. E. Fuller for viscosity measurements; and J. Chen, J. Galperin, P. A. Ware, C. A. Urbston, and M. J. Halfhill for technical assistance.

18 November 1998; accepted 17 February 1999

Hydrogen Peroxide on the Surface of Europa

R. W. Carlson,[1]* M. S. Anderson,[1] R. E. Johnson,[2] W. D. Smythe,[1] A. R. Hendrix,[3] C. A. Barth,[3] L. A. Soderblom,[4] G. B. Hansen,[5] T. B. McCord,[5] J. B. Dalton,[6] R. N. Clark,[6] J. H. Shirley,[1] A. C. Ocampo,[1] D. L. Matson[1]

Spatially resolved infrared and ultraviolet wavelength spectra of Europa's leading, anti-jovian quadrant observed from the Galileo spacecraft show absorption features resulting from hydrogen peroxide. Comparisons with laboratory measurements indicate surface hydrogen peroxide concentrations of about 0.13 percent, by number, relative to water ice. The inferred abundance is consistent with radiolytic production of hydrogen peroxide by intense energetic particle bombardment and demonstrates that Europa's surface chemistry is dominated by radiolysis.

The composition of a planetary surface is an important indicator of its evolution and subsequent chemical alteration. Europa's surface composition can be modified by extrusion of material from the interior (*1*), the infall of cometary and meteoritic material, photochemical processes, and by the deposition of material from the magnetosphere (*2*, *3*). Europa is subjected to intense bombardment by jovian magnetospheric particles—energetic electrons, protons, sulfur ions, and oxygen ions (*4*)—that could alter the composition through radiolysis (*5*, *6*). The relative importance of these chemical alteration processes has not been established for Europa.

Spectra of Europa indicate a water-ice surface (*7*) with sulfur dioxide (SO_2) (*2*, *8*) and hydrated minerals (*9*). The SO_2 could be produced by sulfate decomposition (*10*) or from implanted sulfur ions (*2*). The hydrated minerals may be evaporite salts (*9*), from brine extruded from a hypothetical subsurface ocean (*11*). Infrared (IR) spectra of Europa obtained by Galileo's near-infrared mapping spectrometer (NIMS) (*12*) showed absorption features (*13*) at wavelengths of 4.25, 4.03, and 3.50 μm. Carbon dioxide and SO_2 were identified (*13*) as the 4.25- and 4.03-μm absorbers, similar to previous findings for Ganymede and Callisto (*14*). We show here that the 3.50-μm feature, corroborated with laboratory measurements and Galileo ultraviolet spectrometer (UVS) (*15*) data, indicates the presence of hydrogen peroxide (H_2O_2), formed in this environment by energetic plasma irradiation of Europa's surface (*6*).

NIMS reflectance spectra (Fig. 1A) of Europa's leading anti-jovian quadrant (*16*) show characteristic features of water frost and a feature at 3.50 μm that is not due to H_2O. Hydrocarbons and ammonium-containing minerals were suggested to account for this feature (*13*), but such identifications are problematic because their absorption wavelengths do not match that observed, and both classes of compounds exhibit additional, stronger absorption features not evident in the NIMS spectra. For example, methanol (*17*) shows an absorption band at 3.53 μm and four other strong bands at 3.38, 3.35, 3.14, and 3.04 μm that are not apparent in Europa's spectrum (Fig. 1A). Similar arguments rule out other simple hydrocarbons and ammonium-bearing minerals (*18*). A more likely candidate for the 3.50-μm feature is H_2O_2, which produces $2\nu_2$, $\nu_2+\nu_6$, and $2\nu_6$ combination-bending-mode absorption (*19*, *20*) at ~3.5 μm and has been predicted to occur on icy satellite surfaces (*6*).

For comparison to the NIMS data, we measured (*21*) the diffuse reflectance of H_2O_2 mixtures in water ice and found a band at 3.504 μm (Fig. 1B). Previous measurements (*22*) of UV-photolyzed, 10 K water ice showed the H_2O_2 feature at 3.509 μm, and it shifts to 3.505 μm at 70 K. These wavelengths are consistent with the Europa feature (3.50 ± 0.015 μm). The widths of the Europa and laboratory feature are also consistent, both being ~0.06 μm wide (full width at half maximum) (Fig. 1). With the exception of this feature, frozen aqueous H_2O_2 solutions produce near-IR spectra that are indistinguishable from those of pure water ice.

An estimate of the surface concentration of H_2O_2 is obtained by laboratory IR-reflectance measurements of frozen H_2O_2-H_2O solutions at various concentrations (*21*). Comparing the relative band depths of these spectra with the NIMS spectrum, we find a concentration on Europa of ~0.13 ± 0.07% (by number of H_2O_2 molecules, relative to H_2O; this convention is used throughout) (*21*). The estimate pertains to Europa's 3.5-μm-wavelength, optically sensed surface layer, which is limited by water spectral absorption to depths of about the ice-grain size (*23*), ignoring porosity. The grain size (~60 μm) was determined with the observed IR reflectance factor (*24*) and radiative-transfer calculations for ice-grain surfaces (*25*).

Condensed H_2O_2 in Europa's surface may exist as a solid-state solution in ice or as crystals of pure H_2O_2 or $H_2O_2 \cdot 2H_2O$ (*20*). However, the wavelength (3.52 μm) of the crystalline phases (at 4 and 80 K) is larger than the wavelength of Europa's feature and outside the range allowed by the estimated wavelength uncertainty. Pure amorphous H_2O_2 is precluded because its absorption band occurs at 3.56 μm (*20*).

Hydrogen peroxide absorbs UV radiation (*26*), so if our identification is correct we expect (*6*) a corresponding absorption signature to be present in Galileo UVS spectra (*27*). Disk-resolved UVS measurements (obtained concurrently with the NIMS observations) were com-

[1]Jet Propulsion Laboratory, California Institute of Technology, Pasadena, CA 91109, USA. [2]Engineering Physics, University of Virginia, Charlottesville, VA 22903–2442, USA. [3]Laboratory for Atmospheric and Space Physics, University of Colorado, Boulder, CO 80309–0590, USA. [4]United Stated Geological Survey, Flagstaff, AZ 86001, USA. [5]Planetary Geosciences Division, University of Hawaii, Honolulu, HI 96822, USA. [6]United States Geological Survey, Denver, CO 80225, USA.

*To whom correspondence should be addressed at Mail Stop 183-601, Jet Propulsion Laboratory, 4800 Oak Grove Drive, Pasadena, CA 91109, USA. E-mail: rcarlson@lively.jpl.nasa.gov

pared with the diffuse reflectance of a frozen 0.16% solution of H_2O_2 in water (*28*). The spectra (Fig. 2) are consistent, both showing the onset of absorption at about 300 nm and exhibiting similar shapes at shorter wavelengths. The similarity of these spectra supports the IR identification of H_2O_2 on Europa's surface. However, numerous materials exhibit broad-band UV absorption spectra, so the UV measurements alone do not provide unique identification.

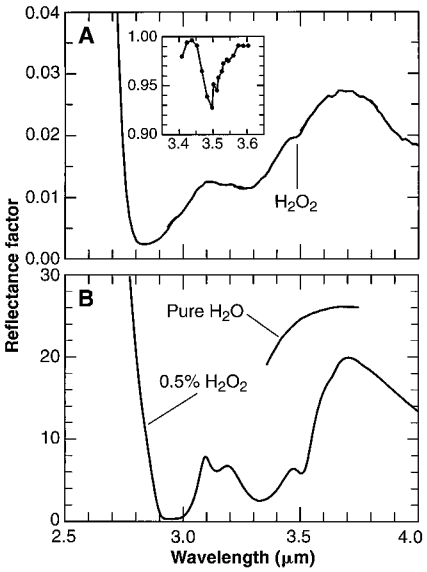

Fig. 1. (**A**) Representative reflectance factor spectrum of Europa's leading, anti-jovian quadrant. The feature at 3.50 μm, identified as H_2O_2 absorption, is shown in the inset as the ratio to the interpolated continuum (the reflectance factor if H_2O_2 were absent). All other structure is due to water; the peak at 3.1 μm is a H_2O restrahlen reflection feature. This spectrum is an average of nine individual spectra, covering 105°W to 125°W, 22°S to 2°N. The 3.50-μm band is found from <100°W to >140°W. (**B**) Laboratory diffuse reflectance spectrum (in percent) of a 0.5% frozen solution of H_2O_2 in water. Combination-bending transitions of H_2O_2 appear at 3.504 μm. No water absorption band occurs at this wavelength, as shown in the pure water ice curve (rescaled). Sample temperatures were 80 K.

The concentration used for the laboratory measurements is about the same as the Europa value, but the grain size, which also affects the reflectivity, was not determined for this laboratory sample, so we cannot independently deduce H_2O_2 concentrations from these UV data. Instead, we used the IR-derived grain size and H_2O_2 UV absorption cross sections (*26*, *29*) to compute theoretical reflectance factor spectra (*25*) for various concentrations of H_2O_2. Comparing these computed reflectance factors with the Europa UV spectrum (Fig. 2) shows that the UVS observations are consistent with the IR-derived abundance for wavelengths less than 250 nm. At longer wavelengths, the observed reflectance is higher than the theoretical values; this could be due to the use of 296 K, liquid-phase absorption coefficients in the calculations, which may be inaccurate for H_2O_2 in low-temperature ice.

Production of H_2O_2 on Europa may be initiated through dissociation of surface water molecules into H + OH by the incident energetic plasma (*6*). Diffusion and chemical combination of two OH radicals yields H_2O_2. Reactive scattering of H and OH by water to form H_2O_2 also may occur (*30*). The energetic particle's energy flux (*31*) is $\Phi \approx 5 \times 10^{10}$ keV s^{-1} cm^{-2}, and each 100 eV of energy will produce $G \approx 0.4$ H_2O_2 molecules, on the basis of results for α-particles (*32*). Solar UV radiation may also dissociate H_2O, but the average dissociating UV energy flux is <1% of that from the energetic particles (*33*). With the above parameters, the production rate of H_2O_2 is $G\,\Phi \approx 2 \times 10^{11}$ molecules s^{-1} cm^{-2}. The incident particles can also destroy H_2O_2 molecules, either by direct dissociation or by production of H, which then reacts with H_2O_2 (*34*). We estimate the rate of destruction of H_2O_2 by the energetic particles using the flux (*31*) $\varphi \approx 1.2 \times 10^8$ s^{-1} cm^{-2} and an assumed cross section of $\sigma = 1 \times 10^{-15}$ cm^2, which is the molecular size of H_2O_2. This gives a loss rate of $\sigma\,\varphi \approx 1.2 \times 10^{-7}$ s^{-1}. Absorption of solar UV radiation, particularly in the 210- to 300-nm region, dissociates H_2O_2 molecules with a diurnally averaged rate of 2.5×10^{-6} s^{-1} (gas phase value) (*33*) and is effective to depths >250 μm (*23*). We ignore the recombination of the spatially contained dissociation products (the cage effect), which can reduce photon-induced loss by a factor of >3 (*35*). The net loss rate will therefore be (2.6 to 0.12) $\times 10^{-6}$ s^{-1} (lifetimes ~ 4 days and ~100 days, respectively), implying surface densities from (0.08 to 1.7) $\times 10^{18}$ cm^{-2}. The vertical stopping distance for energetic electrons (at 60° incidence angle) is about 180 μm (*31*), and less for ions, so the average H_2O_2 concentration in this ~180-μm-deep radiolysis layer will be (0.4 to 9) $\times 10^{19}$ cm^{-3}, or 0.013 to 0.3% relative to water ice. These estimated limits and our derived concentration of 0.13% are consistent.

The abundance of H_2O_2, and the existence of a Na and O_2 atmosphere (*3*, *36*), thought to be produced by energetic-particle bombardment of the surface (*3*, *10*, *36*), demonstrate that surface chemistry on Europa is dominated by radiolysis. At the energy influx rates used above, the optically sensed surface layer can be completely modified in a few tens of years. Temporal changes in the jovian magnetospheric energetic plasma can alter Europa's H_2O_2 abundance, thereby changing Europa's 210- to 300-nm reflectance; such changes have been observed in Europa's UV reflectance (*37*). Because CO_2 and SO_2 are present, themselves the possible products of radiolysis (*10*), related products such as H_2SO_4 and various carbon compounds should be investigated. Predictions, characterization, and identifications of surface species on Europa must consider radiolysis effects.

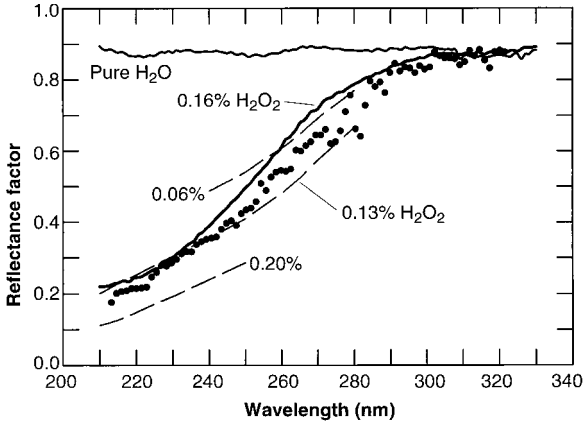

Fig. 2. Europa UV reflectance factor compared with laboratory diffuse reflectance measurements and theoretical values. The Galileo UVS spectrum (●) is an average for longitudes 100°W to 140°W and was obtained simultaneously with the NIMS observations. The laboratory spectra (solid lines) are for a 0.16% H_2O_2 solution and a pure water-ice sample, both at 80 K. Each was measured relative to an aluminum mirror and collectively normalized to Europa data at long wavelengths. Theoretical reflectance factors (dashed lines) were computed for the IR-derived H_2O_2 concentration (0.13 ± 0.07%) and grain size (60 μm).

References and Notes

1. R. Greeley *et al.*, *Icarus* **135**, 4 (1998).
2. A. L. Lane, R. M. Nelson, D. L. Matson, *Nature* **292**, 38 (1981).
3. M. E. Brown and R. E. Hill, *ibid.* **380**, 229 (1996).
4. W. H. Ip, D. J. Williams, R. W. McEntire, B. H. Mauk, *Geophys. Res. Lett.* **25**, 829 (1998).
5. R. E. Johnson, *Energetic Charged-particle Interactions with Atmospheres and Surfaces* (Springer-Verlag, Berlin, 1990).
6. R. E. Johnson and T. I. Quickenden, *J. Geophys. Res.* **102**, 10985 (1997).
7. W. M. Calvin, R. N. Clark, R. H. Brown, J. R. Spencer, *ibid.* **100**, 19041 (1995).
8. K. S. Noll, H. A. Weaver, A. M. Gonella, *ibid.*, p. 19057.
9. T. B. McCord *et al.*, *Science* **280**, 1242 (1998); T. B. McCord *et al.*, *J. Geophys. Res.*, in press.
10. R. E. Johnson, R. M. Killen, J. H. Waite, W. S. Lewis, *Geophys. Res. Lett.* **25**, 3257 (1998).
11. M. H. Carr *et al.*, *Nature* **391**, 363 (1998).
12. R. W. Carlson *et al.*, *Space Sci. Rev.* **60**, 457 (1992).
13. W. D. Smythe *et al.*, paper presented at the 29th Lunar and Planetary Science Conference, Houston, TX, 16 to 20 March 1998 (Lunar and Planetary Institute, Houston, TX, 1998).
14. R. Carlson *et al.*, *Science* **274**, 385 (1996); T. B. McCord *et al.*, *ibid.* **278**, 271 (1997); T. B. McCord *et al.*, *J. Geophys. Res.* **103**, 8603 (1998).
15. C. W. Hord *et al.*, *Space Sci. Rev.* **60**, 503 (1992).
16. The measurements were obtained on 6 November 1997, when Galileo was 480,000 km from Europa. The orbital phase angle and subsolar longitude were 89°, and the subspacecraft longitude was 152°.
17. D. M. Hudgins, S. A. Sandford, L. J. Allamandola, A. Tielens, *Astrophys. J. Suppl.* **86**, 713 (1993).

Arctic Ozone Loss Due to Denitrification

A. E. Waibel,[1]* Th. Peter,[1]† K. S. Carslaw,[1]‡ H. Oelhaf,[2] G. Wetzel,[2] P. J. Crutzen,[1] U. Pöschl,[1]§ A. Tsias,[1] E. Reimer,[3] H. Fischer[1]

Measurements from the winter of 1994–95 indicating removal of total reactive nitrogen from the Arctic stratosphere by particle sedimentation were used to constrain a microphysical model. The model suggests that denitrification is caused predominantly by nitric acid trihydrate particles in small number densities. The denitrification is shown to increase Arctic ozone loss substantially. Sensitivity studies indicate that the Arctic stratosphere is currently at a threshold of denitrification. This implies that future stratospheric cooling, induced by an increase in the anthropogenic carbon dioxide burden, is likely to enhance denitrification and to delay until late in the next century the return of Arctic stratospheric ozone to preindustrial values.

As a result of international regulations, tropospheric chlorofluorocarbon (CFC) concentrations have started to decline (*1*) and stratospheric concentrations are expected to follow with a time delay of 3 to 5 years (*2*). It is therefore expected that the severe chlorine-catalyzed ozone losses that have occurred over the Antarctic and more recently also over the Arctic (*3, 4*) will gradually disappear, although this process may take several decades.

Recent Arctic ozone losses have been associated with particularly low temperatures, as in the winters 1992–93, 1994–95, 1995–96, and 1996–97 (*5*). Reduction of odd nitrogen (NO_x = NO + NO_2) concentrations in the gas phase is an important factor in determining the severity of ozone destruction (*6*). This NO_x reduction may be either temporary via conversion of NO_x into HNO_3 catalyzed by aerosol surfaces (denoxification), or permanent via removal of HNO_3 by sedimenting

[1]Max-Planck-Institut für Chemie, Post Office Box 3060, 55020 Mainz, Germany. [2]Forschungszentrum Karlsruhe, Institut für Meteorologie und Klimaforschung, Post Office Box 3640, D-76021 Karlsruhe, Germany. [3]FU Berlin, Institut für Meteorologie, Carl-Heinrich-Becker-Weg 6-10, D-12165 Berlin, Germany.

*Present address: Lufthansa Systems, FRA4E/DCS, Hugo-Eckner-Ring, D-60549 Frankfurt, Germany.
†To whom correspondence should be addressed. Present address: Institute for Atmospheric Sciences, ETH Zürich, HPP Hönggerberg, CH-8093 Zürich, Switzerland. E-mail: thomas.peter@atmos.umnw.ethz.ch
‡Present address: Environment Centre, University of Leeds, Leeds LS2 9JT, UK.
§Present address: Institut für Wasserchemie, TU München, Marchioninistraβe 17, D-81377 München, Germany.

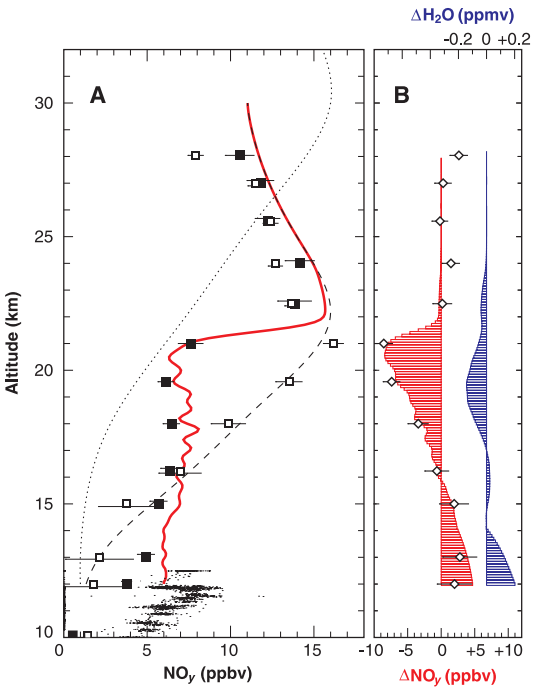

Fig. 1. (**A**) Arctic NO_y profiles in mid-February 1995. Symbols: squares, balloon-borne MIPAS-B observations (*12*); dots, aircraft-borne observations (*16*). Solid symbols are NO_y measurements; open symbols mark NO_y^* deduced from MIPAS N_2O measurements (*13*). NO_y^* represents the unperturbed case (without denitrification). The model calculations are denoted by lines [dotted line, mid-latitude reference NO_y profile (*28*); dashed line, scenario 0 with subsidence of air only (no particle sedimentation); red line, scenario 3 showing the effect of denitrification due to sedimenting ice and NAT particles]. (**B**) Vertical redistribution of NO_y (red) and H_2O (blue). In addition, measured ΔNO_y is shown (◇).

18. R. N. Clark, G. A. Swayze, A. Gallagher, T. V. V. King, W. M. Calvin, "The U.S. Geological Survey Digital Spectral Library: Version 1: 0.2 to 3.0 μm," U.S. Geological Survey Open File Report 93-592.
19. O. Bain and P. A. Giguere, *Can. J. Chem.* **33**, 527 (1955); R. L. Miller and D. F. Hornig, *J. Chem. Phys.* **34**, 265 (1961).
20. P. A. Giguere and K. B. Harvey, *J. Mol. Spectrosc.* **3**, 36 (1959).
21. We measured IR diffuse-reflectance spectra for frozen (~80 K) aqueous solutions of H_2O_2 at concentrations of 0, 0.5, 1, and 1.5%. The solution contained spectrally neutral diamond powder, producing a matte surface without specular reflection. Ice grain sizes were 5 to 15 μm. The factor relating concentration and relative band depth was found after correcting for the minor dependence of relative band depth on grain size, determined from radiative-transfer calculations (*25*). Grain sizes were estimated by comparing measured and computed IR reflectivities. The fractional standard error for the derived factor is 15%. We assume that the band depth is invariant with temperature; the behavior of ice bands [W. M. Grundy and B. Schmitt, *J. Geophys. Res.* **103**. 25809 (1998)] indicates that errors of ±20% are possible. Considering other error sources, the uncertainty in the derived H_2O_2 abundance is estimated to be ±50.
22. P. A. Gerakines, W. A. Schutte, P. Ehrenfreund, *Astron. Astrophys.* **312**, 289 (1996).
23. We adopt, for the effective penetration depth, that level for which the optical depth for equivalent isotropic scatterers is unity. Using similarity relations [B. Hapke, *Theory of Reflectance and Emittance Spectroscopy* (Cambridge Univ. Press, Cambridge, 1993), p. 197] with computed single-scattering albedos and asymmetry parameters (*25*), we find penetration depths for a nonporous medium of 60-μm ice grains of about 60, 250, and 500 μm for wavelengths of 3.5 μm, 210 nm, and 300 nm, respectively.
24. The reflectance factor is the ratio of the observed radiance to that of a perfectly diffuse plane reflector illuminated at the same geometry [B. Hapke (*23*), p. 262].
25. R. W. Carlson and T. Arakelian [*Antarctic J. U. S.* **28**, 256 (1993)] outline the computational method. We used UV and IR optical constants from S. G. Warren [*Appl. Opt.* **23**, 1206 (1984)] and J. E. Bertie, H. J. Labbé, and E. Whalley [*J. Chem. Phys.* **50**, 4501 (1969)], respectively.
26. C. L. Lin, N. K. Rohatgi, W. B. DeMore, *Geophys. Res. Lett.* **5**, 113 (1978).
27. A. R. Hendrix, C. A. Barth, C. W. Hord, A. L. Lane, *Icarus* **135**, 79 (1998).
28. Samples 3 mm thick were frozen, forming granular, diffusing surfaces. The diffuse reflectance was measured, avoiding specular reflection. The UV and IR laboratory measurements were performed at the JPL Vibrational Spectroscopy Laboratory with the use of an Analect diffuse-reflectance attachment with Bio-Rad FTS 6000 and Cary 5E spectrometers.
29. The 3.4 × 10^{-4} M data from (*26*) were used.
30. M. T. Sieger, W. C. Simpson, T. M. Orlando, *Nature* **394**, 554 (1998).
31. We used electron and ion fluxes (for an unmagnetized body at Europa's orbit) and stopping depths in ice from J. F. Cooper, R. E. Johnson, B. H. Mauk, and N. Gehrels (*Icarus*, in preparation). Ion fluxes were increased by a factor of 2 for the finite gyroradius effect (*4*).
32. M. Cottin and M. Lefort, *J. Chim. Phys.* **52**, 545 (1955). Measurements for other particles are needed.
33. W. F. Huebner, J. J. Keady, S. P. Lyon, *Astrophys. Space Sci.* **195**, 1 (1992).
34. J. A. Ghormley and A. C. Stewart, *J. Am. Chem. Soc.* **78**, 2934 (1956).
35. R. Schriever, M. Chergui, N. Schwentner, *J. Phys. Chem.* **95**, 6124 (1991).
36. D. T. Hall, D. F. Strobel, P. D. Feldman, M. A. McGrath, H. A. Weaver, *Nature* **373**, 677 (1995).
37. D. L. Domingue and A. L. Lane, *Geophys. Res. Lett.* **25**, 4421 (1998).
38. Portions of the work described herein were performed at the Jet Propulsion Laboratory, California Institute of Technology, under contract to the National Aeronautics and Space Administration.

11 January 1999; accepted 22 February 1999